Eur Radiol (2004) 14:1990–1998
DOI 10.1007/s00330-004-2446-6

A. Noel
F. Thibault

Digital detectors for mammography: the technical challenges

Received: 16 February 2004
Revised: 2 July 2004
Accepted: 8 July 2004
Published online: 8 October 2004

A. Noel
Centre Alexis Vautrin,
Unité de Radiophysique Médicale,
Paris, France

F. Thibault (✉)
Service de Radiologie,
Institut Curie,
26 rue d'Ulm, 75248 Paris Cedex 05,
France
e-mail: fabienne.thibault@curie.net
Tel.: +33-1-44324200
Fax: +33-1-44324015

Abstract This paper reviews the different techniques available and competing for full-field digital mammography. The detectors are described in their principles: photostimulable storage phosphor plates inserted as a cassette in a conventional mammography unit, dedicated active matrix detectors (i.e., flat-panel, thin-film transistor-based detectors) and scanning systems, using indirect and direct X-ray conversion. The main parameters that characterize the performances of the current systems and influence the quality of digital images are briefly explained: spatial resolution, detective quantum efficiency and modulation transfer function. Overall performances are often the result of compromises in the choice of technology.

Keywords Mammography · Digital radiography · Computed radiography

Introduction

The production of analog or digital mammography images is based on two distinct concepts of image formation. The screen-film system provides a large, continuous sensitive surface with a high resolution. By definition, digital mammography systems use spatial signal sampling that on the contrary limits image resolution. The screen-film system is directly sensitive to the impact of X-rays and stores a visual trace of this impact as a latent image after exposure. However, this capability of both recording and displaying the image has a drawback: while the detection of X-rays requires broad exposure latitude that limits the image contrast, image readability on the contrary requires a high contrast [1]. These two opposite requirements lead to compromises for the choice of the screen-film combination defined once and for all by its characteristic curve [2]. In a digital system on the other hand, image acquisition and display are two independent processes with the advantage of a generally linear response between the intensity of transmitted X-rays and the electronic signal recorded by the system (wide dynamic range). The image display can be optimized by adjustment of the display curve (linear or non-linear, window settings) before printing the film or during visualization on the monitor [1, 2].

The physical properties of the digital image (contrast, resolution and noise) can vary noticeably according to the detection technology used [3–5]. The high level of performance required in mammography is a challenge for digital technology [6]. In this article, we will review the principles of the various types of detectors used for

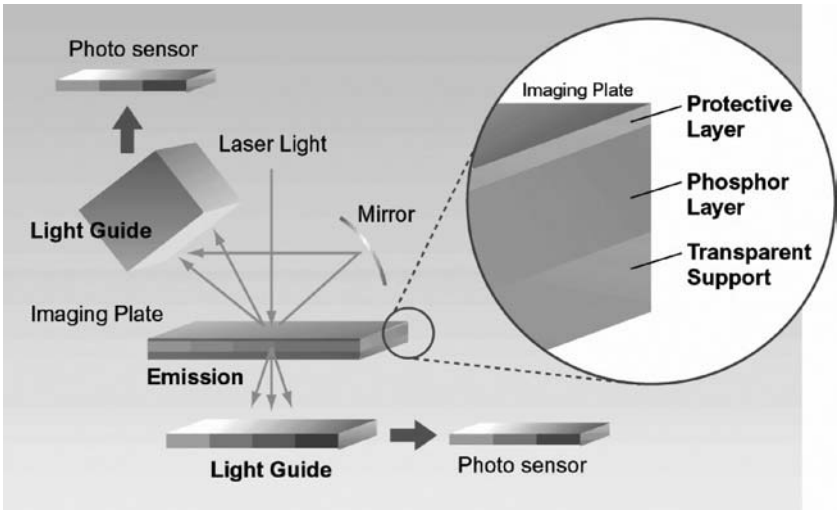

Fig. 1 Principle of simultaneous dual side reading of the photostimulable screen by means of a transparent support. Courtesy of Fuji Medical Systems, France

this specific application. The main parameters that characterize the performances of current dedicated systems and influence the quality of digital images will be explained. A glossary of the terms commonly used for the description of digital imaging systems is added to this article. The terms defined in the glossary are indicated with an asterisk (*).

Available technologies

Three broad classes of detectors are currently available for full-field digital mammography: photostimulable storage phosphors (PSP), active matrix detectors and scanning systems [7]. The two latter categories use either indirect or direct conversion of X-ray photons into electronic charges.

Photostimulable storage phosphors

This removable detector is inserted as a cassette in a conventional mammography unit. Its concept is similar to that of the intensifying screen used in analog mammography. Conventional intensifying screen irradiation induces a change of the energy state of the electrons of the crystalline network from a baseline energy state to an excited state. The number of excited electrons is proportional to the irradiation on each point of the screen. Spontaneous return of these electrons to the fundamental state is accompanied by the emission of a light proportional to the number of excited electrons (i.e., to the irradiation).

With PSP plates [8, 9], the excited electrons are trapped into the crystalline structure where they remain stable for some time. After exposure, a laser beam of appropriate wavelength releases the trapped electrons, inducing the emission of light (i.e., photostimulation). The light emitted at each point of the PSP plate is obtained by scanning the screen with the laser beam. Light is collected then converted into an electrical signal and amplified by a photomultiplier before digital conversion [10].

This type of detector has been used for several years in radiology. Recent developments in the structure of the components [11] have improved the performance of these systems so that PSP plates can now be used in mammography. In the current Fuji system (Fig. 1), light collection is strongly improved by the use of a transparent support that permits readout of both surfaces of the photostimulable screen [12]. The spatial resolution is 50 μm for the 18×24-cm^2 and 24×30-cm^2 available fields of view.

Full-field active matrix detectors

This dedicated flat-panel, thin-film transistor-based detector is integrated into the digital mammography unit. Figure 2 illustrates both indirect and direct conversion.

Indirect conversion

Indirect conversion detectors [13, 14] use a scintillator, which converts the absorbed X-rays into visible light photons. These photons are then converted into electronic charges using an amorphous silicon (a-Si) photodiode* matrix before analog-to-digital conversion. As in other clinical applications [15, 16], current technology for breast imaging [17, 18] uses structured scintillators, typically cesium iodide (CsI). Phosphor crystals within the scintillator form needle-like elements that channel the light emitted onto the photosensitive elements, thereby reducing the lateral spread of visible light (Fig. 3). The spatial resolution obtained with the General Electric system is 100 μm for a 19×23-cm^2 field of view.

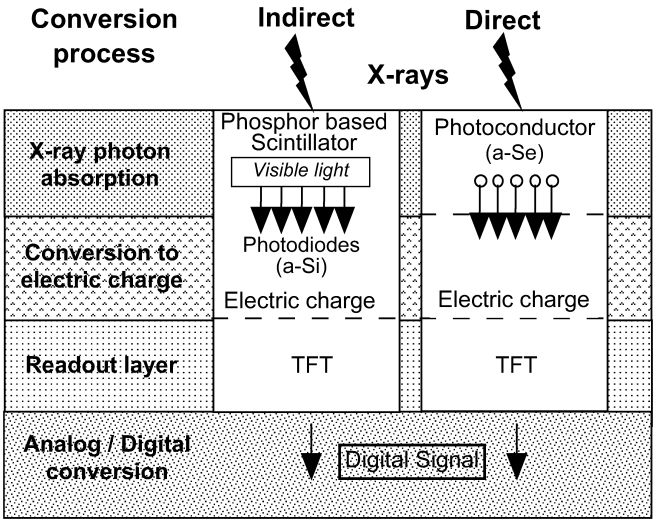

Fig. 2 Modified from Chotas [4]: signal conversion principle for full field active matrix detectors: with indirect-amorphous silicon (a-Si) detectors, as with direct-amorphous selenium (a-Se) detectors, electronic charges are accumulated after X-ray exposure, then read out by arrays of thin-film transistor (TFT*) switches before analog-to-digital signal conversion

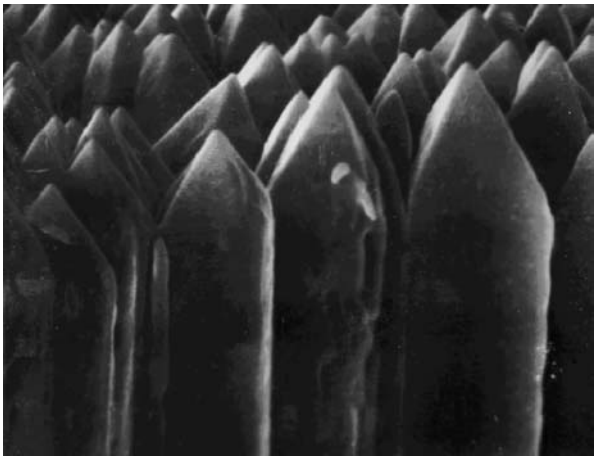

Fig. 3 Light photons are guided through the needle-like structure (about 5 µm in diameter each) of the scintillating crystal onto the photosensitive elements (photodiodes) of the detector. Courtesy of General Electric Medical Systems, France

Direct conversion

Direct conversion detectors [13] use a photoconductive material, typically amorphous selenium (a-Se), that converts the absorbed photons into electronic charges [4, 19, 20–22]. The interaction of X-ray photons with amorphous selenium creates electron-hole pairs producing an electrical current through a bias voltage [4, 13]. Amorphous selenium has a good intrinsic spatial resolution, and this technology is well mastered [21, 23, 24] as amorphous selenium was used in radiology in the 1970s for xeroradiography [25]. Selenium is still used today in photocopiers. The spatial resolution obtained with the a-Se technology commercialized by several manufacturers is 70 µm for a 24×29-cm^2 field of view (Lorad-Hologic, Siemens, Agfa), or 85 µm for a 17.4×23.9-cm^2 field of view (IMS Giotto, Instrumentarium Imaging).

Scanning systems

Data are acquired by simultaneous scanning of the breast by a highly collimated X-ray beam and by the detector [1, 26–28]. With this geometry, only a fraction of the emitted X-ray output is used at each step of the exposure process so that the load for the X-ray tube is higher. Tungsten-target X-ray tubes with high heat storage capacity have been specifically designed for clinical application [26–28]. Because of the reduction of scattered radiation through beam collimation, these systems operate without a grid, which permits a reduction of the dose to the patient. This type of detector provides a high spatial resolution with pixel size of 50 µm or less.

Two scanning mammography systems are currently available. One uses an indirect conversion detector (the Fischer Imaging SenoScan) and the other a direct conversion detector acting as a photon counter (the Sectra MicroDose Mammography).

Indirect conversion “slot-scanning” system

The X-ray beam is collimated to the active area of the detector (Fig. 4). The system uses a 10×221-mm detector with a scintillator coupled by optical fibers to a linear array of four charged-coupled devices (CCDs; Fig. 5a). The optical coupling is direct without reduction. The system comprises groups of 5-µm fibers per 25-µm pixel (Fig. 5b).

Signal measurement is performed by the time delay integration (TDI) method [1, 27]; continuous measurement of the signal at each point of the object examined is performed throughout slot-scanning, which increases the resulting signal. The effective exposure at a given point depends on the value of the current in the tube and on the slot-scanning time. Total scanning time for the entire field of view is 5–6 s, but each point is only irradiated for 200 ms. This technique requires a precise synchronization of the mechanical scanning system and readout electronics to avoid blurring and artifacts. The spatial resolution is 54 µm for a 21×29-cm^2 field of view and 27 µm for a 11×15-cm^2 field of view.

Like in the previous a-Si and a-Se full-field systems, the detector uses an integration process: the signal intensity in each pixel is proportional to the incident energy (transmitted X-rays) [29, 30]. This analog signal is then

Fig. 4 Principle of the slot-scanning system using a highly collimated fan beam that covers the active area of the detector. Data are acquired by simultaneous scanning of the breast by the X-ray beam and the detector, both attached to a pivoting arm in the gantry of the digital unit. The movement of the detector inside the mammography unit (*front view*) is represented in transparency. Courtesy of Fischer Imaging, France

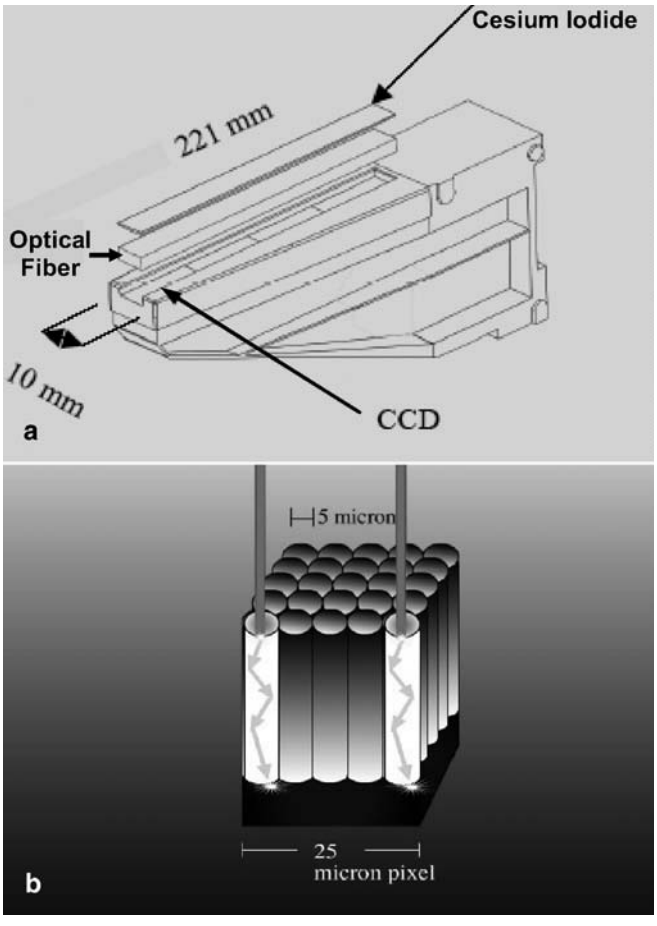

Fig. 5 **a** The 10×221-mm detector in the SenoScan is composed of a scintillator coupled by optical fibers to a linear array of four CCDs. Courtesy of Fischer Imaging, France. **b** Details of the fiber optic coupling module without demagnification, consisting of an array of 5×5 optic fibers (pixel size, 25 μm). Courtesy of Fischer Imaging, France

converted into a digital signal (Fig. 6). The readout electronics of the system is simple, but the detector and the reading system both generate noise. In general, the mean energy absorbed during the interaction of an X-ray photon with the detector varies against the energy of that photon so that low-energy photons make less contribution to forming the image (less signal recorded by the detector) than high-energy photons. Inversely, the informative content of low-energy photons with regard to image contrast is higher due to their increased attenuation. With low-energy photons the signal recorded in each pixel of the receptor is lower than with high-energy photons; a higher irradiation is required for a good image quality [30].

Direct conversion "multi-slit" scanning system

Sectra Imtec AB has recently developed a scanning system composed of several linear slits covering individual pixel rows. The detector consists of a thick layer of crystalline silicon with high absorption capacity. The X-ray interaction creates electron-hole pairs that produce an electrical signal. This direct conversion detector is used as a photon counter [31–33] that distinguishes individual X-ray photons. The resultant pixel size is 50 μm, and the field of view is 26 cm×24 cm.

In this mode, the signal intensity in each pixel is proportional not to the incident energy, but to the number of X-ray photons counted (Fig. 6). Counting the photons can be regarded as an X-ray imaging system that increases the contribution of low-energy photons to the formation of the image. Such a process is an improvement compared to the classical integration process [28]. Only photon-matter interactions above a given energy level are counted by the detector. This system eliminates the noise from the detector and associated electronics, whose level is lower than this cut-off value, but its disadvantage is the complex readout electronics. With this system, the only noise source is the fundamental uncertainty in the

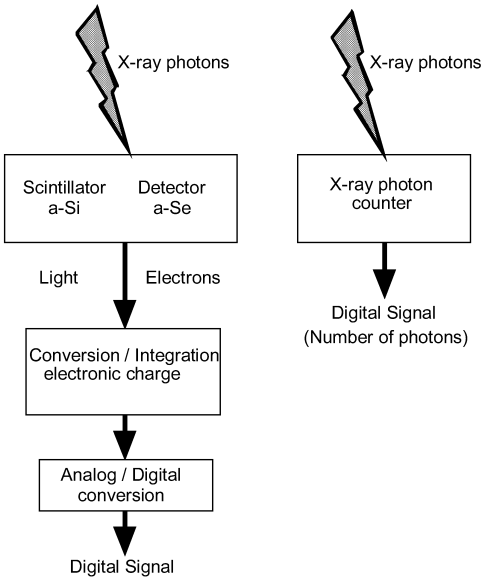

Fig. 6 Diagram of signal integration and photon counting detection technologies

statistical distribution of the incident X-ray photons (i.e., the number of detected photons). The imaging system is said to be "quantum limited" [29, 30]. With a pixel size of 50 µm (10 lp/mm), Sectra asserts that good quality imaging is obtained for 1/5 of the usual doses [34, 35].

Parameters determining the performance of the detector

Spatial resolution

Spatial resolution* determines the dimensions of the smallest visible object. It is measured under special high contrast and low noise test conditions using a low kilovoltage and a high mA s value [29, 30, 36, 37]. These measuring conditions are therefore very different from the exposure parameters used in the diagnostic setting. A higher spatial resolution improves image sharpness. It allows better detection of small details in the image. In particular, a higher spatial resolution improves the morphological analysis of microcalcifications.

Nyquist frequency

The maximum spatial resolution that can be visualized in an image is defined by the Nyquist frequency* (also called cut-off frequency) of the detector calculated from the pixel size, specifically the center-to-center spacing between pixels or pitch [29, 37].

According to Nyquist's sampling theorem, the cut-off frequency is equal to:

$$f_N(line\,pairs/mm) = [1/2 \times pixel\,size\,(mm)]$$

In practice, this means that a detector with a pixel size of 100 µm has a cut-off frequency of 5 line pairs/mm. Objects smaller than 200 µm are therefore not detected. Visualization of smaller objects requires a detector with a smaller pixel size, i.e., with a higher cut-off frequency.

Modulation transfer function (MTF)

MTF* characterizes an additional aspect of the detector's performance. The MTF quantifies the loss of contrast in the image of a given object related to use of this detector [29, 30, 32, 33, 36–38]. The MTF is conditioned by the physical properties of the detector, so that two different detectors may have different MTFs. Loss of contrast depends on the dimensions of the object X-rayed, i.e., the spatial frequencies contained in the image between 0 and the cut-off frequency of the detector. The MTF varies between 1 and 0, where 1 corresponds to complete transmission of the contrast of the object over the entire grey scale of the image and 0 corresponds to no transmission of this contrast, i.e., loss of visualization of this object. By definition, the MTF of an imaging system is equal to 1 for zero spatial frequency. MTF decreases as spatial frequencies in the image increase, but is independent of the pixel size.

Detective quantum efficiency (DQE)

DQE* expresses the efficiency with which a detector uses the incident photons to form an image. DQE is influenced by the noise generated by the detector and by its spatial resolution [29, 32, 33, 36, 37]. The DQE of an ideal detector would be equal to 1: all X-ray photons reaching the surface of the detector would be used to form the image, and this detector would not generate any noise. The DQE of a real detector is less than 1 and reflects degradation of the signal-to-noise ratio (SNR) occurring between the detector input and output:

$$DQE = (SNR_{out}/SNR_{in})^2 \quad 0 \leqslant DQE \leqslant 1$$

DQE depends on spatial frequency. In general, the higher the spatial frequency, the lower the detector output signal and the higher the noise. This process leads to a reduction of the SNR at the detector output, and therefore to a reduction of the DQE of the system.

Compromises and performances

Spatial resolution and pixel size

The maximum spatial resolution visualized in an image is equal to the Nyquist frequency, which is inversely pro-

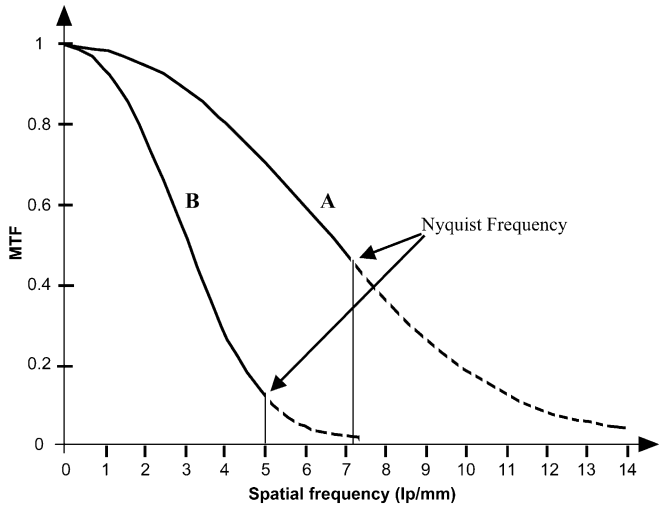

Fig. 7 MTF curves for two types of detectors A and B with different pixel sizes, 70 µm for A and 100 µm for B, respectively. Detector A displays a better MTF at all spatial frequencies than does detector B. Higher spatial resolution is provided by system A with higher Nyquist (cut-off) frequency (7.2 lp/mm). Lower spatial resolution is provided by system B with lower Nyquist frequency (5 lp/mm). Changing the pixel size in B from 100 to 70 µm would raise the cut-off frequency of the system from 5 to 7.2 lp/mm, the shape of the MTF curve being unchanged

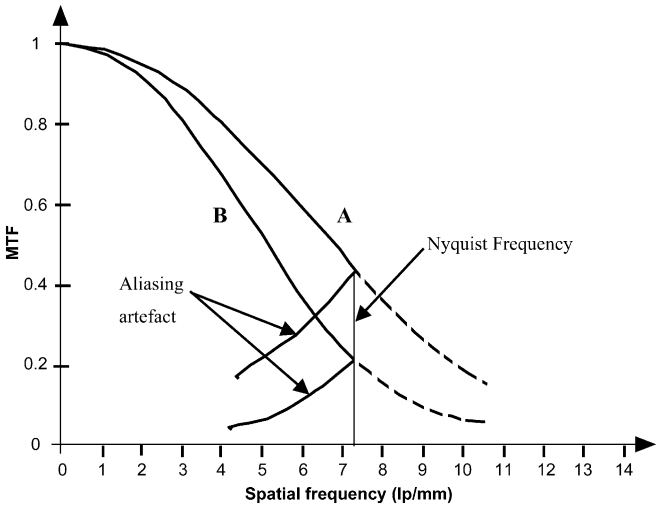

Fig. 8 MTF curves for two imaging systems with the same pixel size of 100 µm, hence the same Nyquist (cut-off) frequency (7.2 lp/mm). System A that exhibits a higher MTF at the Nyquist frequency than system B is prone to more aliasing artifacts

portional to the pixel size: a small pixel size corresponds to a high cut-off frequency and a large pixel size to a low cut-off frequency (Fig. 7). Objects or details of objects with a spatial frequency higher than the cut-off frequency are visualized in the form of artifacts superimposed on lower frequency objects. This phenomenon is called aliasing*.

According to the sampling theorem, the size of the smallest object detectable by digital imaging without aliasing is equal to twice the pixel size of the detector [29, 30]. The aliasing effect can be easily identified on bar-pattern images obtained with line-pair phantom [39]. On mammograms, aliasing should be regarded as an additional source of noise in the image that affects the signal-to-noise ratio, hence the detection process.

When comparing two detectors with different MTFs but the same pixel size, the aliasing effect is stronger for the detector with the highest MTF, i.e., the detector that provides a better contrast transmission at the cut-off frequency, but also non-negligible transmission beyond that frequency. In order to eliminate aliasing, the MTF of the ideal detector should be equal to zero beyond its Nyquist frequency (Fig. 8), which is obviously not possible. This means that for a real detector, the better the MTF, the higher the required Nyquist frequency, i.e., the higher the spatial resolution to be reached to limit the aliasing phenomenon.

Finally, the size of the image matrix (in megabytes) increases as the pixel size decreases. As a result, the memory size occupied by the image is larger. For small pixels (≤85 µm) and given the size and resolution of current diagnostic monitors (i.e., 2×2.5-K for a total of 5 million pixels), the whole image cannot be visualized with full resolution. This requires successive visualization of parts of the image. At this point, one may underline the importance of the image processing step for clinical use [40]. The method of display of digital mammography with a dedicated workstation for soft-copy interpretation is also a crucial issue regarding the effective use of this technique in routine practice [6, 41].

Detective quantum efficiency and spatial resolution

Why is it important to obtain a better DQE?

Image quality depends on the SNR. A reduction of noise improves the detection of low contrast objects in the image, i.e., small and/or low contrast masses. Noise is inversely proportional to the square root of the number of photons collected to form the image [29, 30, 32, 33, 37]. The SNR can therefore be improved either by increasing the number of incident photons (through a higher mA s value), together with an increase in the dose to the patient, or by using a larger portion of the photons reaching the detector, which increases the DQE. A better DQE improves image quality without increasing the dose to the patient, or even by decreasing this dose.

DQE is improved by using thicker detectors or materials with a higher attenuation coefficient (µ). New photoconductor elements will be available in the future: cadmium zinc telluride (CdZnTe) [42], lead iodide (PbI_2),

mercury iodide (HgI_2) [43] and gallium arsenide (GaAs) [44]. The use of iodine in PSPs (BaFI:Eu) has increased the attenuation coefficient of the plates, resulting in a considerable improvement of the DQE (from 19 to about 22%) of these detectors [11].

How to increase DQE without altering spatial resolution?

Although a thicker detection medium increases the X-ray absorption, the consequence is a loss of spatial resolution due to higher scattering. With phosphor-based (i.e., indirect conversion) detectors, the emitted light spreads laterally in proportion to the scintillator thickness. Structured scintillators, which limit this effect, increase the DQE while maintaining spatial resolution. For a-Se direct conversion detectors, an electrical field channels the electronic charges, thus limiting their side scattering.

Direct conversion or indirect conversion

In indirect conversion detectors, the intermediate light production before obtaining electronic charges may reduce the information [45]. Therefore, direct conversion detectors are very efficient. These can capture a very narrow signal profile, which improves the MTF, and hence the quality of the image. The potential drawback is to increase the aliasing* phenomenon when using a detector with a low Nyquist frequency. As explained above, the higher the MTF of the system, the smaller the pixel size needed to avoid aliasing.

Conclusion

Currently, various approaches exist to produce digital detectors for mammography. Each technology presents specific advantages and disadvantages that must be taken into account to optimize examination protocols. The radiologist's objective is to obtain accurate diagnostic information with an acceptable radiation dose to the patient. Overall performances are often the result of compromises in the choice of technology. Digital technologies for breast imaging are rapidly evolving. Large-scale evaluation of this new imaging modality is currently under way in North America, including extensive technical and clinical assessment. At the same time, quality control protocols are being elaborated in the European Union [46] and should also contribute to the spreading of digital mammography.

Glossary

Photodiode (or light-sensitive diode) Semi-conductor element converting light energy into electrical current. The intensity of the current generated, and therefore the quantity of electricity produced, are proportional to the light intensity (itself proportional to the incident irradiation). In the case of indirect conversion detectors, the electronic charges produced are stored in a condenser. Detectors contain one photodiode per pixel.

Thin-film transistor (TFT) Electronic component of an active matrix in which each element (one element per pixel) acts like a switch integrated in the reading circuit to determine the quantity of electronic charges produced by the photodiode and stored in the condenser.

Charge coupled device (CCD) Electronic component converting light energy into electrical current. The quantity of electricity produced, proportional to the light intensity, is stored directly in the device. CCDs are used in indirect conversion detectors.

Structured scintillator Scintillator whose crystalline structure is composed of needle-like elements that channel light down the length of the crystal and minimize lateral spread.

Spatial resolution Spatial resolution is expressed in cycles per mm or, more commonly, in line-pairs per millimeter (lp/mm) and indicates the size of the smallest structure detectable on a test object measured under laboratory conditions, which increase contrast while reducing noise. It is measured by X-raying a phantom composed of periodic elements (alternating bars and spaces) of increasing frequency (bars of decreasing thickness).

Nyquist (or cut-off) frequency Corresponds to a particular value of spatial resolution defined by the pixel size of the digital detector. According to the sampling theorem, the Nyquist frequency is equal to $1/[2 \times \text{pixel size (mm)}]$. It is expressed in lp/mm. Objects with a spatial frequency higher than the Nyquist frequency will either not be visualized or will be visualized incorrectly (aliasing).

Modulation transfer function (MTF) Describe the ability of an imaging system to transfer the contrast of a structure to the final recorded image. In practice, this reflects the loss of contrast induced by the imaging system as a function of spatial resolution, i.e., spatial frequency expressed in line-pairs per millimeter. By definition, the MTF is equal to 1 for a spatial frequency of zero and decreases as far as 0 with increasing spatial frequency.

Spatial frequency The frequency spectrum of an image can be obtained by its Fourier transform. More simply, by analogy with a periodic vibratory phenomenon specified by its frequency (number of cycles per unit of time, usually expressed in hertz, Hz), a pattern in the image is characterized by its repetition in space ex-

pressed in cycles or line-pairs per unit of length. An object with dimension d (for example, d=0.08 mm) contained in the image would be associated with a spatial frequency of 1/2d (1/2×0.08=6.25 lp/mm).

Aliasing Phenomenon resulting from signal undersampling by a digital imaging system, either the detector or reading system (PSP laser beam). Objects with a spatial frequency higher than the Nyquist frequency of the imaging system are replicated as artifacts around the Nyquist frequency that superimpose on objects with lower frequencies. The low frequency noise level is therefore increased, which degrades low contrast object detection.

Detective quantum efficiency (DQE) DQE characterizes the ability of a detector to use the transmitted photons (through the breast, bucky and grid) at the detector input. It is expressed as the ratio of the squares of the signal-to-noise ratio at the detector input and detector output. An ideal system, which would not add any noise, i.e., which would use all photons reaching the detector, would have a DQE equal to 1. A real detector is increasingly "better" as its DQE approaches 1. The DQE of a system is maximal for zero spatial frequency and decreases with increasing spatial frequency.

References

1. Feig SA, Yaffe MJ (1995) Digital mammography, computer-aided diagnosis, and telemammography. Radiol Clin North Am 33:1205–1230
2. Haus AG, Yaffe MJ (2000) Screen-film and digital mammography. Image quality and radiation dose considerations. Radiol Clin North Am 38:871–898
3. Yaffe MJ, Rowlands JA (1997) X-ray detectors for digital radiography. Phys Med Biol 42:1–39
4. Chotas HG, Dobbins JT III, Ravin CE (1999) Principles of digital radiography with large area, electronically readable detectors: a review of the basics. Radiology 210:595–599
5. Gould RG (1997) New detector technology. In: Frey GD, Sprawls P (eds) Proceedings of the AAPM summer school. The expanding role of medical physics in diagnostic imaging. Advanced Medical Publishing, Madison, pp 85–105. ISBN 1-888340-09-6
6. D'Orsi CJ (2002) Digital mammography. Curr Womens Health Rep 2:124–127
7. Noel A, Stines J (2003) La mammographie numérique: les capteurs. J Le Sein 13:206–210
8. von Seggern H, Voigt T, Knupfer W, Lange G (1998) Physical model of photostimulated luminescence of X-ray irradiated BaFBr:Eu^{2+}. J Appl Phys 64:1405–1412
9. Yaffe MJ (2000) Digital mammography. In: Beuttel J, Kundel HL, Van Metter RL (eds) Handbook of medical imaging 1. SPIE, Bellingham, pp 329–372
10. Samei E, Seibert JA, Willis CE, Flynn MJ, Mah E, Junck KL (2001) Performance evaluation of computed radiography systems. Med Phys 28:361–371
11. Nakano Y, Gido T, Honda S, Maezawa A, Wakamatsu H, Yanagita T (2002) Improved computed radiography image quality from a BaFI:Eu photostimulable phosphor plate. Med Phys 29:592–597
12. Arakawa S, Yasuda H, Kohda K, Suzuki T (2000) Improvement of image quality in CR mammography by detection of emission from dual sides of an imaging plate. In: Dobbins JT III, Boone JM (eds) Medical imaging 2000: physics of medical imaging. Proceedings of SPIE 3977. SPIE, Bellingham, pp 590–600
13. Cowen AR, Parkin GJ, Hawkridge P (1997) Direct digital mammography image acquisition. Eur Radiol 7:918–930
14. Rahn JT, Lemmi F, Lu JP, Mei P, Apte RB, Street RA, Lujan R, Weisfield RL, Heanue JA (1999) High resolution X-ray imaging using amorphous silicon flat-panel arrays. IEEE Trans Nucl Sci 46:457–461
15. Herrmann A, Bonel H, Stabler A, Kulinna C, Glaser C, Holzknecht N, Geiger B, Schatzl M, Reiser F (2002) Chest imaging with flat-panel detector at low and standard doses: comparison with storage phosphor technology in normal patients. Eur Radiol 12:385–390
16. Kotter E, Langer M (2002) Digital radiography with large-area flat-panel detectors. Eur Radiol 12:2562–2570
17. Muller S (1999) Full-field digital mammography designed as a complete system. Eur J Radiol 31:25–34
18. Berns EA, Hendrick RE, Cutter GR (2003) Optimization of technique factors for a silicon diode array full-field digital mammography system and comparison to screen-film mammography with matched average glandular dose. Med Phys 30:334–340
19. Lee DL, Cheung LK, Palecki EF, Jeromin LS (1996) A discussion on resolution and dynamic range of Se-TFT direct digital radiographic detector. In: Van Metter RL, Beutel J (eds) Medical imaging 1996: physics of medical imaging. Proceedings of SPIE 2708. SPIE, Bellingham, pp 511–522
20. Stone MF, Zhao W, Jacak BV, O'Connor P, Yu B, Rehak P (2002) The X-ray sensitivity of amorphous selenium for mammography. Med Phys 29:319–324
21. Zhao W, Ji WG, Debrie A, Rowlands JA (2003) Imaging performance of amorphous selenium based flat-panel detectors for digital mammography: characterization of a small area prototype detector. Med Phys 30:254–263
22. Polischuk BT, Rougeot H, Wong K, Debrie A, Poliquin E, Hansroul M, Martin JP, Truong TT, Choquette M, Laperriere L, Shukri Z (1999) Direct conversion detector for digital mammography. In: Boone JM, Dobbins JT III (eds) Medical imaging 1999: physics of medical imaging. Proceedings of SPIE 3659. SPIE, Bellingham, pp 417–425
23. Fahrig R, Rowlands JA, Yaffe MJ (1996) X-ray imaging with amorphous selenium: optimal spectra for digital mammography. Med Phys 23:557–567
24. Rowlands JA, Hunter DM, Araj N (1991) X-ray imaging using amorphous selenium: a photoinduced discharge readout method for digital mammography. Med Phys 18:421–431
25. Paulus DD (1980) Xeroradiography: an in-depth review. Crit Rev Diagn Imaging 12:309–384
26. Tesic MM, Fisher Piccaro M, Munier B (1999) Full field digital mammography scanner. Eur J Radiol 31:2–17

27. Besson GM, Koch A, Tesic M, Sottoriva R, Prieur-Drevron P, Munier B, Calais E, De Groot P (2002) Design and evaluation of a slot-scanning full-field digital mammography system. In: Antonuk LE, Yaffe MJ (eds) Medical imaging 2002: physics of medical imaging. Proceedings of SPIE 4682. SPIE, Bellingham, pp 457–468
28. Thunberg SJ, Francke T, Egerstrom J, Eklund M, Ericsson L, Kristoffersson T, Peskov VN, Rantanen J, Sokolov S, Svedenhag P, Ullberg CK, Weber N (2002) Evaluation of a photon counting mammography system. In: Antonuk LE, Yaffe MJ (eds) Medical imaging 2002: physics of medical imaging. Proceedings of SPIE 4682. SPIE, Bellingham, pp 202–208
29. Dainty JC, Shaw R (1974) Medical imaging. Image science. Academic, London. ISBN 0-12-200850-2
30. Hendee WR, Ritenour ER (2002) Medical imaging physics, 4th edn. Wiley, New York. ISBN 0-471-38226-4
31. Lundqvist M, Danielsson M, Cederström B, Chmill V, Chuntonov A, Aslund M (2003) Measurements on a full-field digital mammography system with a photon counting crystalline silicone detector. In: Yaffe MJ, Antonuk LE (eds) Medical imaging 2003: physics of medical imaging. Proceedings of SPIE 5030. SPIE, Bellingham, pp 547–552
32. Lundqvist M (2003) Silicon strip detectors for scanned multi-slit X-ray imaging. PhD Thesis, Kungl Tekniska Högskolan, Fysiska Institutionen, Stockholm. ISBN 91-7283-512-5, ISSN 0280-316X
33. Mikulec B (2000) Single photon detection with semiconductor pixel arrays for medical imaging applications. PhD Thesis, University of Vienna, Austria. CERN-THESIS 2000-021
34. Danielsson M, Bornefalk H, Cederström B, Chmill V, Hasewaga B, Lundqvist M, Nygren D (2000) Dose efficient system for digital mammography. In: Dobbins JT III, Boone JM (eds) Medical Imaging 2000: physics of medical imaging. Proceedings of SPIE 3977. SPIE, Bellingham, pp 239–249
35. Francke T, Eklund M, Ericsson L, Kristoffersson T, Peskov VN, Rantanen J, Sokolov S, Soderman JE, Ullberg CK, Weber N (2001) Dose reduction using photon counting X-ray imaging. In: Antonuk LE, Yaffe MJ (eds) Medical imaging 2001: physics of medical imaging. Proceedings of SPIE 4320. SPIE, Bellingham, pp 127–132
36. Dobbins JT III (1999) Determination of MTF, NPS and DQE in practice. In: Mansson LG (ed) Lectures notes: physics of medical X-ray imaging, European Commission, ERPET Course, Malmö, 8–12 June, pp F1–F8
37. Dobbins JT III (1995) Effect of undersampling on the proper interpretation of modulation transfer function, noise power spectra and noise equivalent quanta of digital imaging systems. Med Phys 22:171–181
38. Moy JP (2000) Signal-to-noise ratio and spatial resolution in X-ray electronic imagers: is the MTF a relevant parameter? Med Phys 27:86–93
39. Albert M, Beideck DJ, Bakic PR, Maidment AD (2002) Aliasing effects in digital images of line-pair phantoms. Med Phys 29:1716–1718
40. Sivaramakrishna R, Obuchowski NA, Chilcote WA, Cardenosa G, Powell KA (2000) Comparing the performance of mammographic enhancement algorithms: a preference study. Am J Roentgenol 175:45–51
41. Pisano ED, Cole EB, Kistner EO, Muller KE, Hemminger BM, Brown ML, Johnston RE, Kuzmiak CM, Braeuning MP, Freimanis RI, Soo MS, Baker JA, Walsh R (2002) Interpretation of digital mammograms: comparison of speed and accuracy of soft-copy versus printed-film display. Radiology 223:483–488
42. Mainprize JG, Ford NL, Yin S, Gordon EE, Hamilton WJ, Tumer TO, Yaffe MJ (2002) A CdZnTe slot-scanned detector for digital mammography. Med Phys 29:2767–2781
43. Street RA, Mulato M, Schieber MM, Hermon H, Shah KS, Bennett PR, Dmitryev Y, Ho J, Lau R, Meerson E, Ready SE, Reisman B, Sado Y, Van Schuylenbergh K, Vilensky AI, Zuck A (2001) Comparative study of PbI2 and HgI2 as direct detector for high-resolution X-ray image sensors. In: Antonuk LE, Yaffe MJ (eds) Medical imaging 2001: physics of medical imaging. Proceedings of SPIE 4320. SPIE, Bellingham, pp 1–12
44. Amendolia SR, Bisogni MG, Bottigli U, Ciocci MA, Delogu P, Dipasquale G, Fantacci ME, Giannelli M, Maestro P, Marzulli VM, Pernigotti E, Rosso V, Stefanini A, Stumbo S (2000) Low contrasting imaging with a aGaAs pixel digital detector. IEEE Trans Nucl Sci 47:1478–1486
45. Samei E, Flynn MJ (2003) An experimental comparison of detector performance for direct and indirect radiography systems. Med Phys 30:608–622
46. van Engen R, Young K, Bosmans H, Thijssen M (2003) Addendum on digital mammography to the European protocol for the quality control of the physical and technical aspects of mammography screening. Version 1, European Commission, November, EUREF office, Nijmegen